PHYSICAL REVIEW B VOLUME 52, NUMBER 12 15 SEPTEMBER 1995-II

Metastability of NbN in the ordered vacancy NbO phase

E.C. Ethridge, S.C. Erwin, and W.E. Pickett
Complex Systems Theory Branch, Naval Research Laboratory, Washington, D.C. 20375
(Received 10 May 1995)

A metastable phase of NbN with superconducting $T_c = 16.4$ K was reported recently by Treece and collaborators. The reported structure of the thin-film sample deviates from the rocksalt ($B1$) NbN structure with 25% ordered vacancies on each sublattice (space group $Pm3m$) and a lattice constant of 4.442 Å. Using full-potential electronic-structure methods, we contrast the electronic structure with that of $B1$ NbN. The calculated energy, 1.00 eV/molecule higher than $B1$ NbN, and calculated lattice constant of 4.214 Å indicate that the new phase must be something other than the ordered stoichiometric $Pm3m$ phase.

Transition-metal nitrides and carbides possess a number of useful electronic and physicochemical properties such as metallicity and superconductivity, extreme hardness and brittleness, as well as high melting points.[1,2] These attributes make them attractive candidates for applications ranging from composite materials to low-temperature electronic devices. Metastable phases of these compounds have recently been implicated as an improvement upon existing materials, showing enhancements in their electronic properties.[2] In the simplest of the metastable phases, the structures deviate from their ideal rocksalt phase, with ordered vacancies on either the metal or nonmetal sublattice or both.

Recently, a new phase of NbN was reported in thin films fabricated on MgO using pulsed laser deposition (PLD).[3] The sample was shown to demonstrate a superconducting critical temperature of 16.4 K and a lattice parameter of 4.442 Å, both somewhat larger than accepted values for rocksalt structure NbN (16 K; 4.378 Å). This new phase of NbN, shown in Fig. 1, deviates from its common $B1$ (rocksalt) structure with 25% ordered vacancies on both sublattices, which also occurs for NbO. The new phase has $Pm3m$ symmetry, and consists of nonpenetrating Nb octahedra and nonpenetrating N octahedra centered at vacancy sites. Both octahedra have fourfold planar coordination at each atomic site and sixfold "coordination" at the vacancy site. While it is intuitive that this system should reflect behavior similar to that found in electronic and structural analyses of metastable binary carbides, nitrides, and oxides, a detailed theoretical analysis of this new phase of NbN has not yet been carried out. This phase is almost 30% less dense than the rocksalt phase, which already suggests strong alterations in the electronic structure. It is the purpose of this paper to characterize the electronic states of this new phase of NbN and, in particular, to understand the effect of the ordered vacancies on the electronic states. In the discussion to follow, detailed comparisons will be made between the vacancy and rocksalt structure, which will be referred to as Nb_3N_3 and Nb_4N_4, respectively. We also report calculations of the equation of state of both phases that appear to be incompatible with the phase as identified.

Density-functional electronic band calculations were carried out for Nb_3N_3 and Nb_4N_4 using a basis set of linear combination of atomic orbitals (LCAO). The exchange-correlation potential was treated within a local-density approximation as parametrized by Perdew and Zunger.[4] Details of this method have been described elsewhere.[5] In each calculation self-consistency was achieved using 20 special **k** points in the irreducible Brillouin zone. The density of states (DOS) was computed by diagonalizing the Hamiltonian at 104 **k** points in the irreducible zone, followed by Fourier interpolation to a denser grid and integration using the linear tetrahedron method. The basis functions were expanded in a set of 17 Gaussian exponents contracted into seven s-type, five p-type, and four d-type functions for Nb, and 12 exponents contracted into three s-type and two p-type functions for N, for a total of 55 LCAO's per NbN unit.

The Nb_4N_4 and Nb_3N_3 band structures are shown in Fig. 2. For purposes of comparison, both calculations were performed in a simple cubic cell using the reported lattice constant of the $Pm3m$ phase. Mulliken population analysis was used to characterize the orbital percentage of each band in both structures.[6] Figure 2 also indicates the orbital character

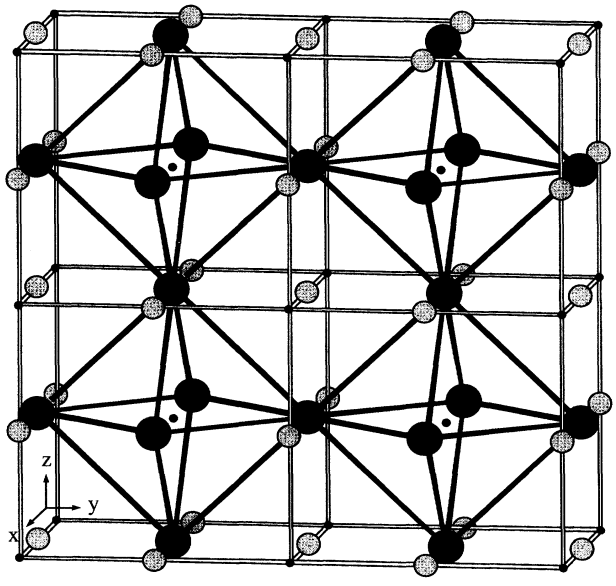

FIG. 1. Crystal structure of Nb_3N_3. Large circles represent Nb sites, small circles represent N sites, and black dots represent vacancy sites. Atom types are interchangeable.

 © 1995 The American Physical Society

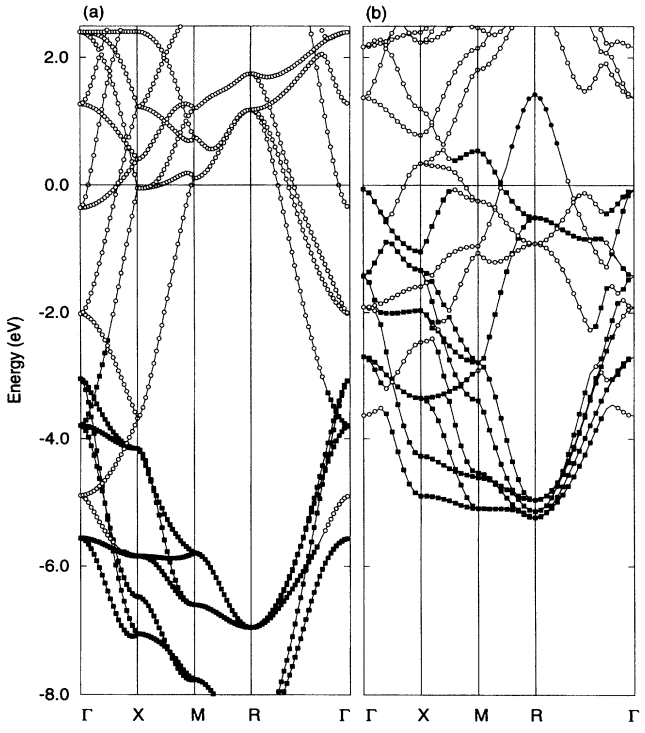

FIG. 2. Self-consistent electronic band structure for (a) Nb_4N_4 and (b) Nb_3N_3. The character of each band, using the method described in the text, is indicated. Filled squares denote N p character, filled circles denote Nb p character, and open circles denote Nb d character. The Fermi level is the energy zero.

of each of the bands, according to the criteria that the Mulliken orbital population of a state exceeds 50%.

In the Nb_4N_4 structure, we observe the type of behavior one has come to expect from IVa and Va metal nitrides in the rocksalt structure.[7] Since each atom is octahedrally coordinated with six atoms of the opposite type, σ bonding may occur between the Nb and N via the a_{1g}, t_{1u}, and e_g orbitals while t_{2g} orbitals comprise the nonbonding orbitals with respect to the Nb-N bonding. The bands near the Fermi level E_F are made up predominantly of Nb states. The Nb bands have mostly t_{2g} symmetry below E_F and are a mixture of e_g and t_{2g} symmetry above E_F. The N p manifold lies below the Nb d bands in the energy range of -8.6 to -3.5 eV. The onset of the Nb p manifold lies above the Nb d near 6 eV.

In the Nb_3N_3 structure, the loss of sixfold coordination gives rise to anisotropic bonding near the vacancy sites that is reflected in a markedly different band structure. Notable features are (1) reduction in the bandwidth by 40% and (2) the presence of a highly dispersive band that crosses the Fermi level and peaks at the R point. This band, referred to as a "vacancy band," is similar to that observed in the isostructural NbO vacancy phase.[8,9] It has Nb d character below E_F and changes to primarily Nb p character as it crosses the Fermi energy. Mulliken population analysis shows that this is the only region for which Nb p states are present within the Nb d complex. The remaining Nb p bands are energetically higher than the Nb d bands. The Fermi level falls in an energy region where both N p and Nb d bands are occupied. The mean energy of the N p band has increased markedly, relative to Nb_4N_4, as is apparent in Fig. 2. These findings are consistent with trends in the vacancy stabilization mechanisms of TiO (Ref. 10) and NbO.[8,9]

The total and partial DOS for Nb_4N_4 is shown in Fig. 3. The peak 5.4 eV below E_F is dominated by N p states with some admixture of Nb d. At higher energies the N p DOS decreases rapidly and contributes very little to the DOS at the Fermi level. Above the Fermi level, a secondary peak is present near 2 eV, which originates from the Nb d states. The onset of this peak occurs below the Fermi level and gives rise to the observed $N(E_F)$ of 3.9 states/eV-sc cell (where sc is simple cubic) with primarily Nb d t_{2g} character.

For the Nb_3N_3 structure, also shown in Fig. 3, $N(E_F)$ is 6.9 states/eV-sc cell, an enhancement relative to its rocksalt counterpart of 75% per unit volume, or 135% per NbN unit. This arises from a dramatic redistribution of the spectral weight of the Nb d bands, which results in a sharply peaked structure at the Fermi level. Although the spectral weight of the the N p bands is shifted to a higher energy, these states are less significant to the enhancement of the DOS at E_F.

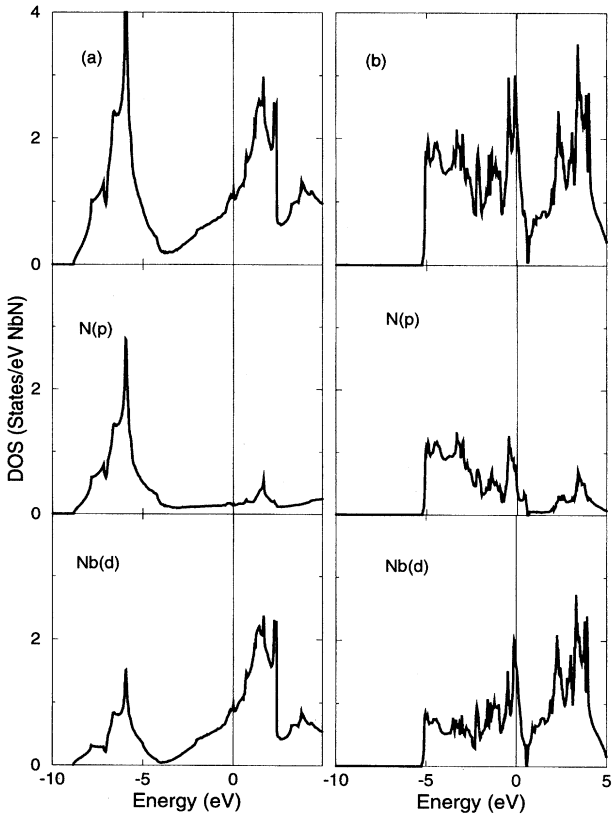

FIG. 3. Density of states (DOS) for (a) Nb_3N_3 and (b) Nb_4N_4 near the Fermi level. For each phase, the top panel shows total DOS, middle and bottom panels show atom- and symmetry-projected partial DOS for nitrogen and niobium, respectively. Contributions from (Nb s and p, N s) states not shown here are negligible. The Fermi level is the energy zero.

TABLE I. Total and decomposed atomic charge distribution of Nb and N in the Nb_4N_4 and Nb_3N_3 phases.

	Nb_4N_4		Nb_3N_3	
	Nb	N	Nb	N
Q	40.17	7.83	40.29	7.71
s	8.18	3.72	8.15	3.77
p	18.15	4.11	18.36	3.94
d	13.84	0	13.78	0
x		1.37		1.38
y		1.37		1.38
z		1.37		1.18
xy	2.88		2.62	
yz	2.88		2.82	
zx	2.88		2.82	
x^2-y^2	2.60		2.68	
$3z^2$	2.60		2.84	

It is instructive to contrast the proposed Nb_3N_3 phase with the isostructural Nb_3O_3. In Nb_3O_3, the Fermi level falls slightly above a pseudogap in the DOS and results in a low $N(E_F)$. The presence of this minimum is considered to be an indication of the stabilization brought about by the ordered vacancies. Andersen and Satpathy[11] have shown that the directed d^4 orbitals introduced by Cotton and Haas[12] constitute a basis for understanding the stability of Nb_3O_3: all bonding orbitals are filled and a single antibonding orbital is occupied. In Nb_3N_3, which has three fewer electrons, two of the bonding orbitals are unoccupied. In addition, the Fermi level falls at a position of large density of states that leaves the uppermost occupied states with high band energy. Both of these effects disfavor the stability of the $Pm3m$ phase for NbN.

To gain insight into the role of the vacancies, effective electron configurations were computed for the constituents of both structures and summarized in Table I. The total (Mulliken) charge on each atom is decomposed according to orbital and symmetry type. The symmetry decomposed charge distribution of Nb_4N_4 reflects the full cubic symmetry of the structure. For Nb_4N_4, the total charge transferred from Nb to N is 0.83. The Nb_3N_3 structure is slightly less ionic with a charge transfer of 0.71. A comparison of the two phases shows that the difference in the ionic charges arises from a reduction in charge transfer from the Nb p to the N p states.

It is useful to define a local coordinate system at each atom with the z axis directed toward a vacancy site (i.e., along the axis of the D_{4h} point group). There are two types of (100) planes. The Nb-rich plane, defined at $y=0.5$ (or equivalently at $x=0.5$) in Fig. 1, is made up of Nb atoms next-nearest-neighbor (nnn) coordinated with Nb atoms. In this plane, the symmetry equivalent Nb xz, yz orbitals are directed at nnn Nb atoms. In the N-rich plane, defined at $z=0$ in Fig.1, Nb atoms are nearest-neighbor (nn) coordinated to N atoms. Niobium xy, x^2-y^2 orbitals are directed at nn N's in this plane and Nb-N $dp\sigma$ bonding is maintained. As shown in Table I, the charge on these Nb orbitals is smaller than the out-of-plane Nb orbitals. This indicates that while charge transfer occurs in this plane due to Nb-N σ bonding, the presence of vacancy sites in adjacent planes reduces the charge transfer in the perpendicular direction.

To ascertain the relative stability of the two phases of NbN we have calculated the equation of state. We have used the full-potential linearized augmented plane-wave method[13,14] (LAPW) with the Vosko-Wilk-Nusair[15] parametrization of the exchange-correlation energy and potential in the local-density approximation. For all calculations sphere radii were taken to be $R_{Nb}=2.30$ a.u. for Nb and $R_N=1.55$ a.u. for N. For Nb_3N_3 empty spheres of the same sizes were placed at the Nb and N vacancies, respectively. The basis set cutoff was defined by $R_N K_{max}=7.0$, which translates to $R_{Nb}K_{max}=10.4$. The basis set size ranged from 760 LAPW's for the smallest volume to 1080 LAPW's for the largest volumes, for the simple cubic cell that was used. The Nb $3p$ semicore states were treated in the same window for additional accuracy that might be necessary at the smaller volumes considered, and additional local functions were used for the Nb $3p$ and $4d$ states and for the N $2s$ states. Twenty special **k** points were used in all calculations.

The calculated energy curves, presented versus the simple cubic lattice constant, are shown for both phases in Fig. 4. There are two unexpected results: (1) the predicted lattice constant for the Nb_3N_3 phase, 4.214 Å, is much smaller than the reported value[2] of 4.442 Å, and (2) the energy of the Nb_3N_3 phase is *1.00 eV higher* per NbN unit than in the rocksalt phase. The calculated lattice constant of the rocksalt phase is 4.365 Å, within 0.3% of the experimental value, lending confidence to our predictions.

Other results from our equation of state include the bulk modulus B and its pressure derivative B': for the Nb_4N_4

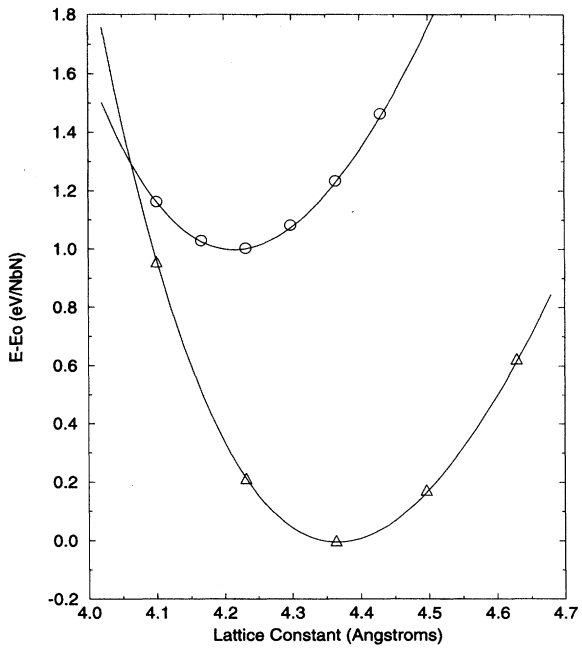

FIG. 4. Theoretical equation of state for Nb_4N_4 (open triangles) and Nb_3N_3 (open circles). Energy is per NbN unit, with the Nb_4N_4 minimum taken as the energy zero. The symbols are calculated values, while the lines represent fits to the Birch equation.

phase $B=3.57$ Mbar, $B'=4.54$; for the Nb_3N_3 phase $B=3.84$ Mbar, $B'=4.38$. These equations of state results are not compatible with the identification of the structure of the PLD NbN film. First, the equilibrium lattice constant is 5% less than the reported one. This could conceivably be rationalized as a sufficiently thin film stabilized in a highly strained film due to epitaxial registry, except that the MgO substrate has a lattice constant (4.21–4.24 Å depending on temperature) that is 5% smaller than the reported value of 4.442 Å. Second, the energy difference of 1.00 eV per NbN unit is exceedingly large, and a 5% strain would increase this difference noticeably. The stored energy in even a few monolayers of the Nb_3N_3 phase could never be sustained by bond formation at the interface.

In summary, we have found that ordered vacancies in NbN play a similar role in the electronic band structure to that observed in isostructural NbO and that the slight charge redistribution among Nb and N atoms could be explained in terms of the structural anisotropy. However, we have calculational evidence that the observed phase cannot be a stoichiometric $Pm3m$ phase of NbN. It is energetically unfavorable (by 1.00 eV/NbN) compared to Nb_4N_4 and the predicted lattice constant is 5% smaller than reported. We are currently searching for an alternative structure for the observed phase.

The authors acknowledge Serdar Öğüt and Karin M. Rabe for useful discussions. E.C.E gratefully acknowledges the National Research Council for financial support.

[1] L.E. Toth, *Transition Metal Carbides and Nitrides* (Academic, New York, 1971).

[2] V.A. Gubanov, A.L. Ivanovsky, and V.P. Zhukov, *Electronic Structure of Refractory Carbides and Nitrides* (Cambridge University Press, Cambridge, England, 1994).

[3] R.E. Treece, J.S. Horwitz, and D.B. Chrisey, in *Polycrystalline Thin Films: Structure, Texture, Properties and Applications*, edited by K. Barmak, M.A. Parker, J.A. Floro, R. Sinclair, and D.A. Smith, MRS Symposia Proceedings No. 343 (Materials Research Society, Pittsburgh, 1994), p. 747; R.E. Treece *et al.*, Appl. Phys. Lett. **65**, 2860 (1994); R.E. Treece, J.S. Horwitz, D.B. Chrisey, and E.P. Donovan, Chem. Mater. **6**, 2205 (1994); R.E. Treece *et al.*, Phys. Rev. B **51**, 9356 (1995).

[4] J.P. Perdew and A. Zunger, Phys. Rev. B **23**, 5048 (1981).

[5] S.C. Erwin, M.R. Pederson, and W.E. Pickett, Phys. Rev. B **41**, 10 437 (1990).

[6] R.S. Mulliken, J. Chem. Phys. **23**, 1833 (1955).

[7] D.A. Papaconstantopoulos, W.E. Pickett, B.M. Klein, and L.L. Boyer, Phys. Rev. B **31**, 752 (1985), and references therein.

[8] E. Wimmer *et al.*, J. Phys. Chem. Solids **43**, 439 (1982).

[9] W.W. Schulz and R.M. Wentzcovitch, Phys. Rev. B **48**, 16 986 (1993).

[10] L.M. Huisman, A.E. Carlson, C.D. Gelatt, Jr., and H. Ehrenreich, Phys. Rev. B **22**, 991 (1980).

[11] O.K. Andersen and S. Satpathy, in *Basic Properties of Binary Oxides*, edited by A. Dominguez Rodriguez, J. Castaing, and R. Marquez [Servicio de Publicationes de la Universidad de Sevilla (Serie Ciencias), Sevilla, 1984], pp. 21–42.

[12] F.A. Cotton and T.E. Haas, Inorg. Chem. **3**, 10 (1964).

[13] D.J. Singh, *Planewaves, Pseudopotentials, and the LAPW Method* (Kluwer, Boston, 1994); Phys. Rev. B **43**, 6388 (1991).

[14] S.H. Wei and H. Krakauer, Phys. Rev. Lett. **55**, 1200 (1985).

[15] S. Vosko, L. Wilk, and M. Nusair, Can. J. Phys. **58**, 1200 (1980).

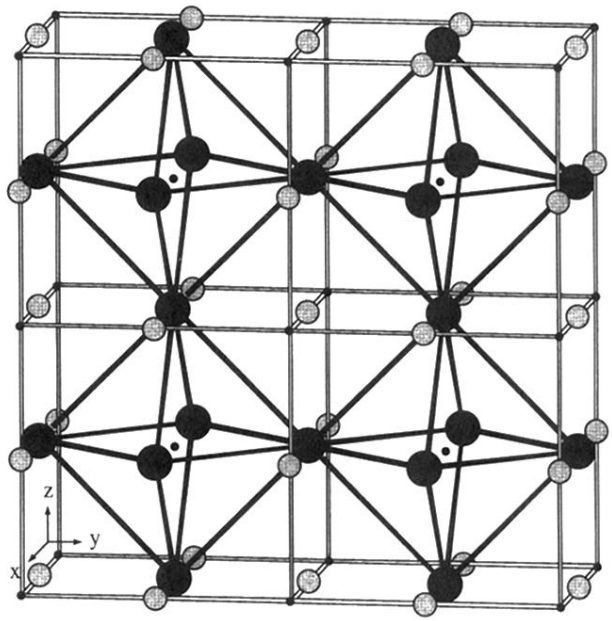

FIG. 1. Crystal structure of Nb_3N_3. Large circles represent Nb sites, small circles represent N sites, and black dots represent vacancy sites. Atom types are interchangeable.